

Modeling and Experimental Analysis of a Wearable Energy Harvester that Exploits Human-Body Motion

Miah A Halim¹, Robert Rantz¹, Qian Zhang², Lei Gu², Ken Yang², and Shad Roundy¹

¹Dept. of Mechanical Engineering, University of Utah, Salt Lake City, UT 84112, USA

²MEMS Development Group, Analog Devices Inc., Wilmington, MA 01887, USA

Email: halim.miah@utah.edu

Abstract— This paper reports modeling and analysis of a wearable rotational energy harvester from human-body motion. Our analysis started with the collection of inertial measurement unit (IMU) data from different human-body locations (wrist, chest, waist, and ankle) at a constant walking speed. Based on the characteristics of the IMU data, a sprung eccentric rotational proof-mass based energy harvesting system has been developed and its mathematical model is derived. The model is used to investigate the electromechanical behavior of the system via numerical simulation and validated experimentally with an electromagnetic (EM) energy harvester prototype. Results indicate that on average the proposed sprung rotational energy harvesting system outperforms its conventional counterpart (without spring) for most of the human-body locations while walking at 3.5 mph on a treadmill.

Keywords—human-body motion; rotational energy harvester; sprung eccentric rotor; electromagnetic transducer

I. INTRODUCTION

Wearable technology (WT) is blooming all over the world with a variety of applications. It appears prominently in consumer electronics with the popularization of the smartwatch and fitness tracker. Apart from consumer uses, WT is being incorporated into navigation systems, e-textiles, and healthcare [1]. However, uninterrupted operation of wearable devices is yet to be achieved due to the limited lifetime of batteries. Batteries for most wearable devices last only a few hours to a few days and require periodic charging. Therefore, there is an urgent need for self-powered wearables.

Typical sources of energy on the human-body include body heat and kinetic energy generated by human-body-induced motion while walking, running or jogging [2,3]. However, a significant difficulty in harvesting energy from human-body-induced motion in a small wearable device is the low-frequency, non-periodic, and unpredictable nature of the motion induced at different body-locations [3]. Due to this unpredictable nature of human-body-induced motion, it is challenging to determine the best functioning structure for a wearable kinetic energy harvester and to predict its power generation capability. Generally, an inertial mechanism in the form of spring-mass-damper system is employed in kinetic energy harvesting in which piezoelectric, electromagnetic, and electrostatic transducers are used for energy conversion [4,5]. Since wearable devices are coupled with the body and have

tightly constrained size and space, the possibilities for wearable energy harvesting systems are more restricted than for many other applications. Therefore, a clever design approach is desirable. Frequency up-conversion and rotational mechanisms are widely adopted techniques for wearable energy harvesting from human-body motion [6-8]. However, the internal travel range of the inertial mass in such energy harvesters is restricted which, in turn, limits power generation.

In this study, we have analyzed the performance of a sprung rotational energy harvester by utilizing IMU data collected from different human-body locations (wrist, chest, waist, and ankle) under a certain walking speed. A mathematical model has been derived to predict the electromechanical behavior and power output of the system. Additionally, experiments are conducted using an EM energy harvester prototype to validate the model predictions.

II. IMU DATA FROM HUMAN-BODY MOTION

In order to design a wearable energy harvester, it is quite important to understand the nature of human-body-induced motion. Different human-body locations (e.g., wrist, arm, chest, hip, knee, ankle etc.) may produce different types of excitations during different activities (e.g., walking, running, jogging, shaking limbs, jumping etc.). In this study, we have relied on measurements of human-body excitation at different locations using 6-axis IMUs (3-axis linear acceleration and 3-axis rotational rate) to model the proposed energy harvesting approach. IMU measurements were performed at a constant walking speed (3.5 mph) on a treadmill by mounting IMU devices (Shimmer 3) on the wrist, chest, waist, and ankle of nine human subjects, as shown in Fig. 1(a). Each IMU device

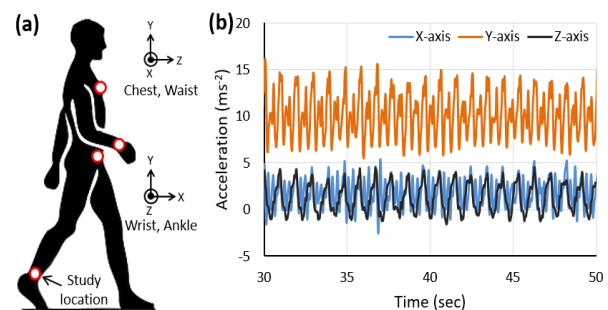


Fig. 1. (a) Study locations on the human-body and (b) sample acceleration waveforms collected from wrist while walking at 3.5 mph on a treadmill.

contains a 3-axis accelerometer whose axis orientation is also indicated in the figure.

Fig.1(b) shows the example waveforms collected from the wrist of one subject which is representative of the acceleration patterns of all the data recorded. Note that the recorded acceleration data include gravitational acceleration as well. The key observation is that the peak-to-peak acceleration is much larger along the vertical (Y) axis than the two (X and Z) other axes. Therefore, the motion amplitude of the inertial mass of a rotational energy harvester is highly influenced along vertical axis, and the harvester should be designed to exploit that fact while still generating power from inputs along the other axes. According to our observation on the collected acceleration data, a conventional (frequency up-converted and rotational) harvester is not effective enough for wearable energy harvesting. Therefore, other concepts, such as a sprung rotational energy harvester must be considered.

III. MODELING OF THE ENERGY HARVESTER

A rotational energy harvester model for human-body motion has been derived based on a generalized three-dimensional model of an eccentric proof-mass rotating freely on a bearing as shown in Fig. 2(a) [9]. It considers 6-axis motion inputs (linear inputs along X , Y , Z and rotational inputs θ_x , θ_y , θ_z to the housing) and system constraints such as the rotational inertia and the eccentricity of the eccentric proof-mass for power generation. It includes both electrical and mechanical dampers (viscous) representing both energy extraction from an ideal transducer and energy losses due to friction, respectively. It is obvious that the rotational and linear excitation inputs work on the system in three-dimensions, however the rotation of the eccentric proof-mass is constrained to motion in the XY plane.

Based on the IMU data analysis discussed earlier, the response (motion in the XY plane) of the eccentric proof-mass to a given excitation is poor as the proof-mass mostly just hangs downward due to the effect of gravity. To improve the performance of the system, a torsional spring is added that couples the eccentric proof-mass to the reference frame. The torsional spring holds the eccentric proof-mass vertically up at $\pi/2$ radians so that its response to excitation along the vertical axis is enhanced. The generalized model for a sprung eccentric rotational system is illustrated in Fig. 2(b). Multiple coordinate frames are represented where X_0Y_0 is an inertial reference

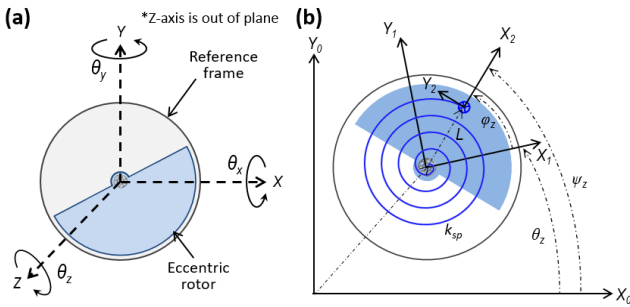


Fig. 2. Schematic representations of (a) an eccentric rotor based rotational energy harvester [9] and (b) generalized model of a sprung eccentric rotor in an inertial reference frame.

frame, X_1Y_1 is a reference frame fixed to the housing of the rotational system, and X_2Y_2 is a reference frame fixed to the rotational inertia about center of gravity. The governing equation of the proposed sprung rotational system can be expressed as [10]

$$\ddot{\varphi}_z = -\frac{mL(\ddot{Y} \cos \varphi_z - \ddot{X} \sin \varphi_z) + (b_m + b_e)\dot{\varphi}_z + k_{sp}(\varphi_z - \pi/2)}{mL^2 + I_g} - \ddot{\theta}_z \quad (1)$$

where m , L , and I_g are the mass of the eccentric rotor, eccentric length and rotational inertia of the rotor about center of gravity, respectively. \ddot{X} and \ddot{Y} are the input accelerations to the system working along X and Y coordinates, respectively. b_m and b_e are the mechanical and electrical damping coefficients, respectively. k_{sp} is the stiffness of the torsional spring. θ_z is the rotational input to the reference frame along Z direction and φ_z is the angular displacement of the rotor relative to the reference frame. The input accelerations (\ddot{X} and \ddot{Y}) are the combination of both linear and gravitational accelerations (recorded by the IMU devices). Then, the average power output (under certain excitation signal of length T) for this generalized sprung rotational system is determined by:

$$P_{avg} = \frac{1}{T} \int_0^T b_e \dot{\varphi}_z^2 dt \quad (2)$$

IV. RESULTS AND DISCUSSION

The model derived earlier has been analyzed numerically and validated by human-body motion of the same human subjects who participated in IMU data collection using a fabricated EM energy harvester prototype (with and without a torsional spring).

A. Numerical Simulation

The electromechanical behavior and output performance of the proposed system have been analyzed by numerically solving Eqn. (1) using MATLAB. The raw IMU data collected from nine human subjects are directly used as inputs. The simulation parameters are shown in Table I. It is observed that the dynamic response of the system is influenced by the stiffness of the torsional spring which in turn affects power generation. Fig. 3 shows simulated average power output as a function of torsional spring stiffness using IMU data collected from wrists of nine subjects while walking at 3.5 mph on a treadmill. In the graph, zero spring stiffness corresponds to the eccentric rotor without spring. Fig. 3 shows that the optimal spring stiffness varies greatly from subject to subject which is because of the unique excitation pattern (uncontrolled, nonperiodic and inconsistency) of each subject. A controlled and periodic excitation would give consistent results [11].

TABLE I. PARAMETERS USED IN NUMERICAL SIMULATION

Parameter	Value
Mass of the eccentric rotor, m	12.14×10^{-3} Kg
Inertia about center of gravity, I_g	10.92×10^{-7} Kg.m ²
Eccentric length, L	1.65×10^{-3} m
Mechanical damping coefficient, b_m	0.72×10^{-6} N.m.s/rad
Electrical damping coefficient, b_e	2.88×10^{-6} N.m.s/rad
Stiffness of the torsional spring, k_{sp}	$0 \sim 4.0 \times 10^{-4}$ N.m/rad

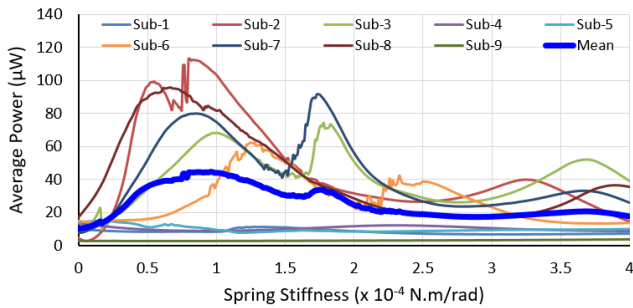


Fig. 3. Simulated average power vs. spring stiffness using the IMU data collected from wrist at 3.5 mph walking speed on treadmill.

However, we have taken the mean values to determine the approximate optimal spring stiffness which is in the range between 0.7×10^{-4} N.m/rad and 1.2×10^{-4} N.m/rad. Similarly, the performances (average power) of both unsprung and sprung systems at different human-body locations have been predicted numerically using corresponding raw IMU data as inputs.

Fig. 4 shows the mean average power of nine human subjects generated at different body locations while walking at 3.5 mph on a treadmill. Note, for each subject an average power over time is calculated as per Eq. 2, the values shown in fig. 4 are the mean of the nine average power values. Results show that the sprung ($k_{sp} = 1.15 \times 10^{-4}$ N.m/rad) rotational system performs significantly better than the unsprung system at wrist, chest and waist locations. However, the performance of the unsprung system at the ankle location is still better. This is due to a relatively higher excitation pulse upon heel strike and leg swing during walking that allows the unsprung rotor to swing freely with higher rotational velocity.

B. Experimental Verification

In order to validate the model, a macro-scale EM rotational energy harvester prototype has been fabricated and tested, as shown in Fig. 5. The EM transducer consists of an array of magnet pole-pairs (with iron backing) incorporated within the eccentric rotor that rotates about the shaft (fixed to the housing) and a series connected coil array (packaged in a PCB) fixed to the housing. Damping coefficients of the prototype (with and without spring) were determined by recording (using high-speed camera) and analyzing the free oscillation of the eccentric rotor after deflecting it (by 90°) from its stable equilibrium position [13].

The prototype (with and without spring) was tested on the

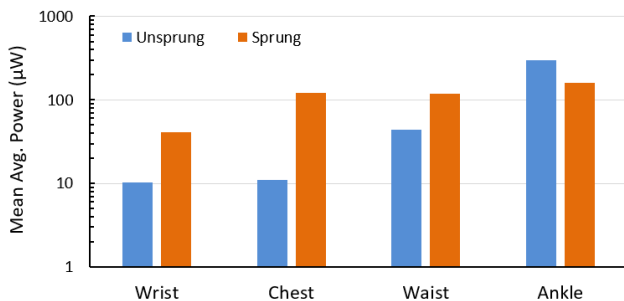


Fig. 4. Simulated mean average power generated by the energy harvester placed at different body locations at 3.5 mph walking speed on a treadmill.

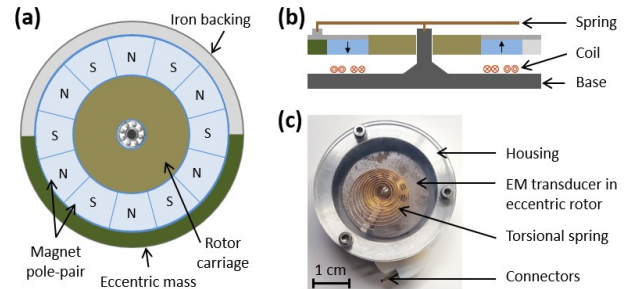


Fig. 5. Conceptual schematics of (a) magnet pole-pairs incorporated in the eccentric rotor and (b) the sprung rotational energy harvester (cross-section). (c) Photograph of a fabricated prototype.

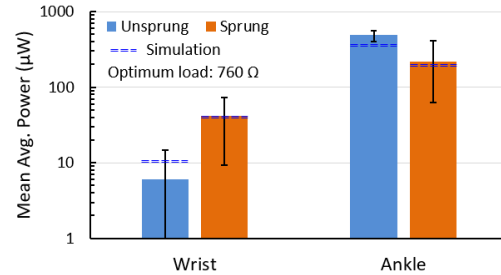


Fig. 6. Measured mean average power generated by the EM energy harvester prototype at different body locations at 3.5 mph walking speed on a treadmill.

same human subjects who participated in IMU data collection, under the same walking condition. An off-the-shelf torsional spring of 1.15×10^{-4} N.m/rad stiffness was chosen. At this stage of our experiment, we have tested the prototype on two different human-body locations (on wrist and ankle. Fig. 6 shows mean values of the average power measured from nine subjects at the wrist and five subjects at the ankle (number of subjects varied due to resource constraints). Experimental results are in good agreement with the simulation results. It is to be noted that we have noticed variation in results (indicated by error bars) from one subject to another due to the unique walking pattern of each subject which is of interest for further analysis.

V. CONCLUSION

We have presented modeling and analysis of a wearable rotational energy harvester for human-body-induced motion. IMU data collected from different human-body locations were used to corroborate the model derived for a sprung rotational energy harvesting system. Numerical analysis shows that a sprung (with approximate optimal spring stiffness) rotational energy harvester outperforms over its conventional counterpart at most of the body locations measured. Experimental results from an EM prototype energy harvester (on wrist and ankle) match the simulation results which validates our mathematical model. Our future work will include further analysis of the proposed system in a broader extent (e.g., more subjects, more body locations, various activities such as running, jogging, office task etc.).

ACKNOWLEDGMENT

This research was funded through a generous grant from Analog Devices Inc.

REFERENCES

- [1] A. Godfrey, V. Hetherington, H. Shum, P. Bonato, N. H. Lovell, and S. Stuart, "From A to Z: Wearable technology explained," *Maturitas*, vol. 113, pp. 40–47, July 2018.
- [2] V. Leonov, "Energy harvesting for self-powered wearable devices" in *Wearable monitoring systems*, Chp. 2, A. Bonfiglio, D. De Rossi, Eds. Springer US, 2011, pp. 27–49.
- [3] Y. M. Choi, M. G. Lee, and Y. Jeon, "Wearable biomechanical energy harvesting technologies," *Energies*, vol. 10, p. 1483, September 2017.
- [4] C. Wei and X. Jing, "A comprehensive review on vibration energy harvesting: Modelling and realization," *Renew. Sust. Energ. Rev.*, vol. 74, pp. 1–18, February 2017.
- [5] J. Siang, M. H. Lim, and M. S. Leong, "Review of vibration - based energy harvesting technology: mechanism and architectural approach," *Int. J. Energy Res.*, vol. 42, pp. 1866–1893, January 2018.
- [6] M. A. Halim, H. Cho, M. Salauddin, and J. Y. Park, "A miniaturized electromagnetic vibration energy harvester using flux-guided magnet stacks for human-body-induced motion," *Sens. Actuators A*, vol. 249, pp. 23–31. August 2016.
- [7] S. Wei, H. Hu, and S. He, "Modeling and experimental investigation of an impact-driven piezoelectric energy harvester from human motion," *Smart Mater. Struct.*, vol. 22, p. 105020, September 2013.
- [8] P. Pillatsch, E.M. Yeatman, and A.S. Holmes, "A piezoelectric frequency up-converting energy harvester with rotating proof mass for human body applications," *Sens. Actuators A*, vol. 206, pp. 178–185, February 2014.
- [9] Q. Zhang, L. Gu, K. Yang, M. A. Halim, R. Rantz, and S. Roundy, "Kinetic energy harvesting using improved eccentric rotor architecture for wearable sensors," *IEEE Sensors Conference'16*, Orlando, FL, pp. 1628–1630, October 2016.
- [10] R. Rantz, M. A. Halim, T. Xue, Q. Zhang, L. Gu, K. Yang, and S. Roundy, "Architectures for wrist worn energy harvesting," *Smart Mater. Struct.*, vol. 27, p. 044001, March 2018.
- [11] M. A. Halim, R. Rantz, Q. Zhang, L. Gu, K. Yang, and S. Roundy, "An electromagnetic rotational energy harvester using sprung eccentric rotor, driven by pseudo-walking motion," *Appl. Energy*, vol. 217, pp. 66–74, March 2018.